

Ab-initio determination of the incommensurate modulated structure of Bi-2212 from x-ray powder diffraction data – a simulation ^{*}

Chen Jian-Rong(陈建荣), Gu Yuan-Xin(古元新),
Zheng Chao-De(郑朝德), and Fan Hai-Fu(范海福)[†]

Institute of Physics, Chinese Academy of Sciences, Beijing 100080, China

(Received 4 April 2003; revised manuscript received 12 May 2003)

A set of x-ray powder diffraction data of the high- T_c superconductor $\text{Bi}_2\text{Sr}_2\text{Ca}_1\text{Cu}_2\text{O}_y$ (Bi-2212) was simulated based on the experimental single-crystal diffraction data by merging together reflections with diffraction angles (2θ) closer to each other than 0.04 degrees. There are three types of overlapping in the powder diffraction data, i.e. (i) overlapping of main reflections; (ii) overlapping of satellite reflections and (iii) overlapping of main and satellite reflections. The third type of overlapping was first separated into main and satellite components according to the ratio between the average intensity of that of types (i) and (ii). Then the overlapped reflections of main reflections and those of the satellites were uniformly partitioned. Heavy-atom sites in the basic/average structure were found using the uniformly decomposed main reflections by the conventional direct method. Phases of the satellites were derived by the multidimensional direct method. The resultant four-dimensional Fourier maps revealed correctly the essential feature of the modulation. No assumption on either the basic structure or the modulation is needed.

Keywords: powder diffraction analysis, incommensurate modulated structures, direct methods

PACC: 6110M

1. Introduction

Multidimensional direct methods have been introduced for *ab-initio* determination of incommensurate modulated structures without relying on any pre-assumed models.^[1] A number of originally unknown incommensurate modulated structures have been solved successfully using multidimensional direct methods with x-ray as well as electron diffraction data from single crystals.^[2–4] However, to prepare single-crystal samples for many important materials such as high- T_c superconductors is often difficult. Therefore, it is interesting to try and see whether multidimensional direct methods are capable of solving incommensurate modulated structures using powder diffraction data. The main difficulty arising from powder diffraction data in comparison with single-crystal diffraction is the overlapping of individual reflections.^[5,6] In the present test we use a set of artificial powder diffraction data, which is simulated from a set of experimental single-crystal diffraction data by merging together reflections with diffraction

angles (2θ) closer to each other than 0.04 degrees.

2. Method

Incommensurate modulated structures do not have three-dimensional (3D) periodicity but can be regarded as a 3D hypersection of a four- or higher-dimensional periodic structure.^[7,8] With this representation, the Sayre equation can be easily extended to multidimensional space.^[1,9] We have the multidimensional Sayre equation similar to that in three-dimensional space, i.e.

$$F(\mathbf{h}) = \frac{\Theta}{V} \sum_{\mathbf{h}'} F(\mathbf{h}') F(\mathbf{h} - \mathbf{h}'), \quad (1)$$

where \mathbf{h} is a multidimensional reciprocal vector defined as

$$\mathbf{h} = h_1 \mathbf{b}_1 + h_2 \mathbf{b}_2 + h_3 \mathbf{b}_3 + \cdots + h_{3+n} \mathbf{b}_{3+n} \quad (n = 1, 2, \cdots), \quad (2)$$

with $h_1, h_2, \cdots, h_{3+n}$ all integers and $\mathbf{b}_1, \mathbf{b}_2, \cdots, \mathbf{b}_{3+n}$ the basic vectors of the multidimensional reciprocal lattice. Θ is an atomic form factor. V is the volume

^{*}Project supported by the National Natural Science Foundation of China, (Grant No 19974068) and the Ministry of Science and Technology of China, (Grant No NKBRF G1999064603).

[†]Correspondence email: fan@aphy.iphy.ac.cn

of the unit cell of the 3D basic structure. The right-hand side of Eq. (1) can be split into three parts, i.e.

$$F(\mathbf{h}) = \frac{\theta}{V} \left\{ \sum_{\mathbf{h}'} F_m(\mathbf{h}') F_m(\mathbf{h} - \mathbf{h}') + 2 \sum_{\mathbf{h}'} F_m(\mathbf{h}') F_s(\mathbf{h} - \mathbf{h}') + \sum_{\mathbf{h}'} F_s(\mathbf{h}') F_s(\mathbf{h} - \mathbf{h}') \right\}. \quad (3)$$

Where the subscript m denotes the main reflections while the subscript s denotes satellites. Since the intensity of satellites is on average much weaker than that of main reflections, the last summation on the right-hand side of Eq. (3) is negligible in comparison with the second one, while the last two summations on the right-hand side of Eq. (3) are negligible in comparison with the first. Letting $F(\mathbf{h})$ on the left-hand side of Eq. (3) represents only the structure factor of main reflections, we have to the first approximation

$$F_m(\mathbf{h}) \approx \frac{\theta}{V} \sum_{\mathbf{h}'} F_m(\mathbf{h}') F_m(\mathbf{h} - \mathbf{h}'). \quad (4)$$

On the other hand, if $F(\mathbf{h})$ on the left-hand side of Eq. (3) corresponds only to satellites, it follows that

$$F_s(\mathbf{h}) \approx \frac{\theta}{V} \sum_{\mathbf{h}'} F_m(\mathbf{h}') F_m(\mathbf{h} - \mathbf{h}') + \frac{2\theta}{V} \sum_{\mathbf{h}'} F_m(\mathbf{h}') F_s(\mathbf{h} - \mathbf{h}'). \quad (5)$$

For incommensurate modulated structures, other than composite structures, the first summation on the right-hand side of Eq. (5) has vanished. Since any 3D reciprocal lattice vectors corresponding to a main reflection will have zero components in the extra dimensions so that the sum of two such lattice vectors could never give rise to a lattice vector corresponding to a satellite. We then have

$$F_s(\mathbf{h}) \approx \frac{2\theta}{V} \sum_{\mathbf{h}'} F_m(\mathbf{h}') F_s(\mathbf{h} - \mathbf{h}'). \quad (6)$$

Eq. (4) indicates that the phase of main reflections can be derived by a conventional direct method neglecting the satellites. Equation (6) can be used to extend phases from main reflections to satellites. This provides an objective way to determine the modulation functions. The procedure consists of the following stages:

i) Derive phases of main reflections using Eq. (4);

ii) Derive phases of satellite reflections using Eq. (6);

iii) Calculate a multidimensional Fourier map using the observed structure-factor magnitudes and the phases from i) and ii);

iv) Cut the resulting Fourier map with a 3D 'hyperplane' to obtain an 'image' of the incommensurate modulated structure in the 3D physical space;

v) Parameters of the modulation functions are measured directly on the multidimensional Fourier map resulting from iii).

The program DIMS (Direct methods for Incommensurate Modulated Structures) has been written for the implementation of steps i) and ii).^[10]

3. Data

The high- T_c superconductor $\text{Bi}_2\text{Sr}_2\text{Ca}_1\text{Cu}_2\text{O}_y$ (Bi-2212) is a one-dimensionally modulated incommensurate structure in the superspace group $N[Bbmb]1-11$ with unit cell parameters of the basic structure $a=0.5422$, $b=0.5437$, $c=3.0537\text{nm}$, $\alpha=\beta=\gamma=90^\circ$ and the modulation wavevector $\mathbf{q}=0.22\mathbf{b}^* + \mathbf{c}^*$. Different authors have independently studied the incommensurate modulation in Bi-2212.^[4] A set of synchrotron x-ray powder diffraction data was simulated based on the experimental single-crystal x-ray diffraction data.^[11] Since the single-crystal data were collected with an in-house x-ray generator using Cu $K\alpha$ radiation ($\lambda=0.15418\text{nm}$), it is reasonable to expect that a set of synchrotron x-ray powder diffraction data could reach the same diffraction limit. Hence we set the resolution limit of the simulated synchrotron x-ray diffraction data to the same as that of the single-crystal data. The FWHM (full width at half maximum) of the simulated powder diffraction data is assumed to be $\Delta(2\theta) \leq 0.04^\circ$. This is adequate since the FWHM of $\Delta(2\theta) \leq 0.025^\circ$ in the range of $30^\circ \leq 2\theta \leq 80^\circ$ have been reported by Wroblewski *et al* as early as in 1988 for synchrotron x-ray powder diffraction.^[12] One may argue that crystals with structural modulation should give broader reflections in comparison with ordinary crystals. However, modulated crystals are not necessarily disordered crystals. In our experiment, single crystals of Bi-2212 yield sharp reflections comparable to that of ordinary crystals. Accordingly in our simulation, reflections are recognized as isolated (unique), if their 2θ -value differ from that of the nearest neighbour more than 0.04° . Others are regarded as overlapped. The resultant artificial powder-diffraction data set contains 1879 reflec-

tions. Since most reflections are overlapped, no phasing attempts were made to unique reflections alone. There are three types of overlapping, i.e. (i) overlapping among main reflections; (ii) overlapping among satellites and (iii) overlapping of main and satellite reflections. Many overlapped reflections are mixers of the three categories. There are 89 of the total 543 main reflections without overlapping with satellites and 295 of the total 1336 satellites without overlapping with main reflections. The third category of overlapping was first separated according to the ratio between the average intensity of the 89 main reflections and that of the 295 satellites. Then the first two kinds of overlapping were treated by uniformly partitioning. We assumed that experimental errors due to preferred orientation, absorption, etc, have been treated properly with available techniques. Hence they were not considered in our test.

4. Phasing main reflections and locating heavy-atom sites in the basic structure

With the 543 decomposed main reflections, a default run of the direct method program SAPI revealed all the heavy atoms of the basic structure on top of the output peak list.^[13] Heavy-atom coordinates from the peak list are shown in Table 1 in comparison with that previously obtained from single-crystal diffraction data.^[11]

5. Phasing satellite reflections

543 main reflections, 867 first-order and 469 second-order satellite reflections were involved in the

Table 1. Coordinates of metal atoms in the basic structure of Bi-2212 found by the program SAPI with the artificial powder diffraction data. Values obtained previously from single-crystal data are in parentheses.

Atom	x	y	z
Bi	0.7579	0.0211	0.0513
	(0.7713)	(0)	(0.0510)
Sr	0.2914	0.0167	0.1327
	(0.2519)	(0)	(0.1382)
Ca	0.2486	0.0150	0.2499
	(0.25)	(0)	(0.25)
Cu	0.7555	0.0082	0.1938
	(0.7494)	(0)	(0.1953)

calculation. Phases calculated from the metal atoms were assigned to main reflections. Phases of satellites were then derived according to Eq. (6) using the multidimensional direct method program DIMS.^[10] In Table 2, there are listed the cumulative phase errors of direct method phasing of powder diffraction data. The errors were calculated against the final model obtained from single-crystal diffraction data. As is seen, the percentage of reflections with their phase (sign) wrongly determined is $\sim 23\%$ for main reflections, $\sim 6\%$ for first-order satellites and $\sim 39\%$ for second-order satellites. The reason of having a somewhat abnormally large phase error for main reflections is that, only metal atoms rather than the whole basic structure that includes oxygen atoms were used in the phase calculation. Nevertheless, the quality of such a set of phases was still sufficient in deriving phases for satellites. The small percentage of wrong signs ($\sim 6\%$) for first-order satellites ensured the correct determination of the modulation waves. The reason of the large phase error for second-order satellites is that they are much weaker reflections in comparison with the first-order satellites.

Table 2. Cumulative distribution of wrong phases (signs) results from direct method phasing (SAPI for main reflections and DIMS for satellites). Reflections are arranged in descending order of F (obs).

Main reflections		First-order satellites		Second-order satellites	
Number of reflections	Number of wrong signs	Number of reflections	Number of wrong signs	Number of reflections	Number of wrong signs
100	14	100	7	100	42
200	36	200	11	200	88
300	60	300	16	300	121
400	84	400	21	400	154
500	110	500	24	469	185
543	124	600	27		
		700	37		
		800	47		
		867	53		

6. Resultant Fourier maps

The four-dimensional Fourier map was calculated using the program VEC (<http://cryst.iphy.ac.cn/VEC/index.html>) with the structure-factor magnitudes of the decomposed main and satellite reflections and phases derived as described above. Figure 1 shows the section of the four-dimensional (4D) Fourier map at $x_1=0.25$ and $x_2=0$.^[14] The upper part shows the result from the powder data, while the lower part shows the result from the single-crystal diffraction data.^[11] The x_4 axis is parallel to the modulation vector \mathbf{q} . A 4D atom without modulation will be a straight bar parallel to the x_4 axis. Positional modulation changes the direction, while compositional modulation changes the width of the bar. As is seen, all the metal-atom "bars" resulting from powder data are changing their direction in the same way as that resulting from the single-crystal data. The same can be seen also in the 3D Fourier map (the hypersection perpendicular to the fourth axis of the 4D Fourier map) projected along the \mathbf{a} axis (see Fig.2). It is seen that the modulation for metal atoms revealed by powder analysis is nearly the same as that from single-crystal analysis. One of the prominent features of modulation in the high- T_c superconductor Bi-2212 found in previous studies is the so-called saw-tooth modulation of the oxygen

atom O_4 .^[11,15,16] Fig. 3 shows the saw-tooth modulation of O_4 revealed by powder analysis in comparison with that from single-crystal analysis. Again we see the consistency between the powder method and the single-crystal method.

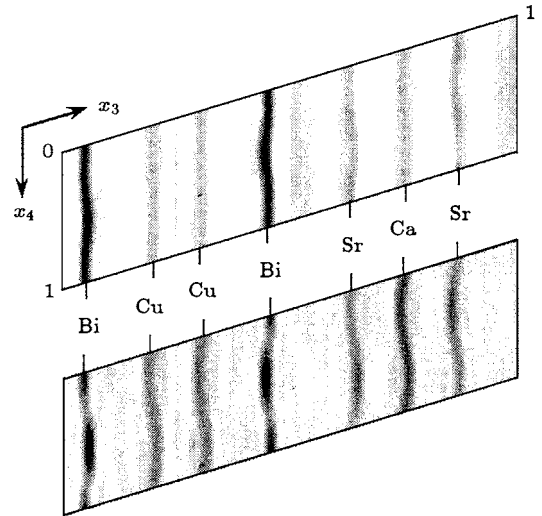


Fig.1. Section of the 4D Fourier map of the Bi-2212 high- T_c superconductor at $x_1=0.25$ and $x_2=0$. The value of electron density is proportional to the grey level on the map. Upper part: resulting from phasing powder diffraction data; Lower part: resulting from single-crystal diffraction data.^[9]

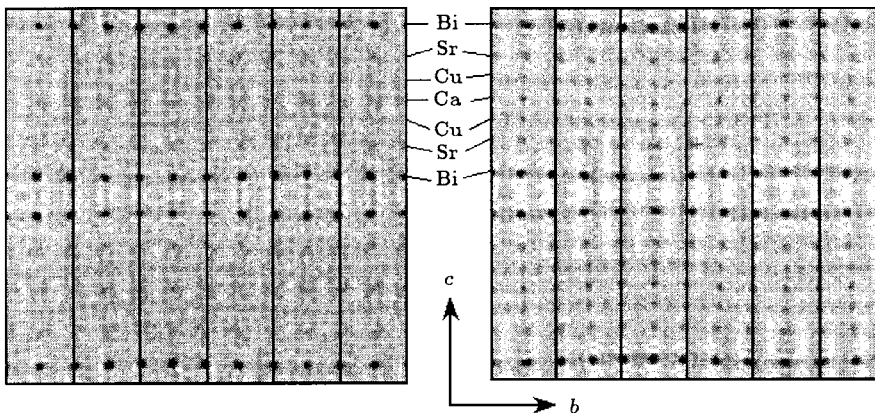


Fig.2. Hypersection perpendicular to the fourth axis of the 4D Fourier map of the high- T_c superconductor Bi-2212 projected down the \mathbf{a} axis. The value of electron density is proportional to the grey level on the map. Six unit cells of the basic structure are plotted along the b axis. Unit-cell borders are shown with black solid lines. Left: result from powder analysis. Right: result from single-crystal analysis.

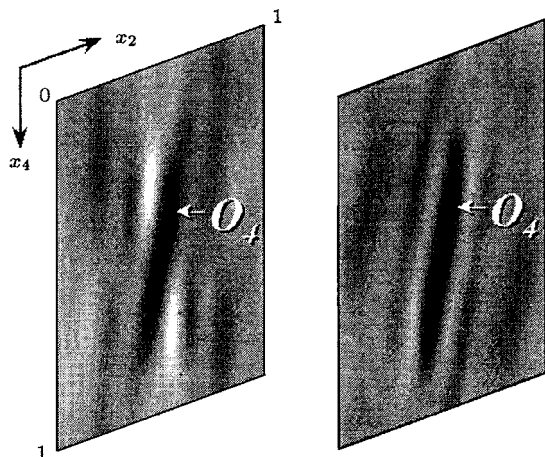


Fig.3. The 2D section of 4D Fourier map of the high- T_c superconductor Bi-2212 cut at $x_1=0.145$ and $x_3=0.058$, showing the saw-tooth modulation of the oxygen atom O_4 . The value of electron density is proportional to the grey level on the map. Left: result from powder analysis. Right: result from single-crystal analysis.

7. Concluding remarks

The simulating test described in this paper showed that multidimensional direct methods are capable of *ab-initio* phasing synchrotron x-ray powder diffraction data of incommensurate modulated crystalline materials. The separation of main and satellite components of overlapping reflections is essential for providing the basic of successful direct method phasing. A simple and effective procedure for this purpose has been proposed in this paper. While results of the present test are adequate for deriving a rough structure model, there is still room for further improvement. Better results can be expected if the known basic structure is available as the starting point of direct method phasing or, if the procedure of partitioning overlapping reflections can be further improved.

References

- [1] Hao Q, Liu Y W and Fan H F 1987 *Acta Cryst. A* **43** 820
- [2] Mo Y D, Cheng T Z, Fan H F, Li J Q, Sha B D, Zheng C D, Li F H and Zhao Z X 1992 *Supercond. Sci. Technol.* **5** 69
- [3] Lam E J W, Beurskens P T, Smits J M M, Van Smaalen S, De Boer J L and Fan H F 1995 *Acta Cryst. B* **51** 779
- [4] Fan H F 1999 *Microscopy Res. Techn.* **46** 104
- [5] Gu Y X, Liu Y D, Hao Q and Fan H F 2000 *Acta Cryst. A* **56** 592
- [6] Chen J R, Gu Y X and Fan H F 2003 *Chin. Phys.* **12** 310
- [7] Wolff P M de 1974 *Acta Cryst. A* **30** 777
- [8] Janner A and Janssen T 1977 *Phys. Rev. B* **15** 643
- [9] Sayre D 1952 *Acta Cryst.* **5** 60
- [10] Fu Z Q and Fan H F 1994 *J. Appl. Cryst.* **27** 124
- [11] Fu Z Q, Li Y, Cheng T Z, Zhang Y H, Gu B L and Fan H F 1995 *Sci. Chin. A* **38** 210
- [12] Wroblewski T, Ihringer J and Maichle J 1988 *Nucl. Instrum. Methods A* **226** 664
- [13] Fan H F, Yao J X, Zheng C D, Gu Y X and Qian J Z 1991 *SAPI: a Computer Program for Automatic Solution of Crystal structures from x-ray Diffraction Data* (Beijing: Institute of Physics, Chinese Academy of Sciences)
- [14] Wan Z H, Liu Y D, Fu Z Q, Li Y, Cheng T Z, Li F H and Fan H F 2003 *Z. Krist.* (in press)
- [15] Petricek V, Gao Y, Lee P and Coppens P 1990 *Phys. Rev. B* **42** 387
- [16] Gao Y, Coppens P Cox D E and Moodenbaugh A R 1993 *Acta Cryst. A* **49** 141